

CHAPTER 17

FUNCTIONAL-STRUCTURAL MODELLING OF CHRYSANTHEMUM

P.H.B. DE VISSER[#], G.W.A.M. VAN DER HEIJDEN[#],
E. HEUVELINK^{##} AND S.M.P. CARVALHO^{##}

[#] *Plant Research International, Wageningen, The Netherlands*

^{##} *Horticultural Production Chains, Wageningen University, Wageningen,
The Netherlands*

Abstract. An integration of structural and physiological models is used to simulate 3D plant growth and visual appearance of cut chrysanthemum, reacting to environmental factors. Measurements to calibrate the model include 3D data of digitized plants as well as a number of measurements and observations on harvested plants, including biomass per organ. The structural module is based on the L-systems algorithm. This L-system calculates temperature- and light-driven development, branching pattern and flower formation. In this 3D-structural model existing rules for physiological processes are incorporated, enabling calculation of carbon dynamics. A 3D radiosity method is used to calculate light absorption of every organ (leaf) at an hourly basis. Hourly photosynthesis per leaf is calculated according to the biochemical model of Farquhar taking into account absorbed light, CO₂ and temperature at hourly intervals. A relative sink-strength approach is used to distribute the available assimilates among organs at a daily basis. Simulation of plant-to-plant competition for light is enabled. The modelling of temperature and light-level effects on growth and flower quality is based on trial data at different temperatures and plant density levels. The model is able to visualize different flower qualities in terms of flower number and branching patterns per plant. The results show the integrative effects of local sinks, specific in time and 3D position, on structure and ornamental quality at plant level.

INTRODUCTION

A number of studies have shown the usefulness of explanatory models in simulating the interactions of climate and management on ornamental quality and quantitative properties of chrysanthemum plants (Larsen and Gertsson 1992; Carvalho and Heuvelink 2003; Lee and Heuvelink 2003). Those models all operate at the plant level, and do not explicitly simulate 3D plant structure although they may be able to discriminate between individual organs using a ranking or index (e.g. Marcelis et al. 2006). Moreover, physiological processes that relate to structure cannot be modelled explicitly, for example light absorption on individual leaves or flow of substances

199

J. Vos, L.F.M. Marcelis, P.H.B. de Visser, P.C. Struik and J.B. Evers (eds.), Functional-Structural Plant Modelling in Crop Production, 199-208.

© 2007 Springer. Printed in the Netherlands.

and signals. Here, we present a prototype functional-structural plant model (FSPM) for cut chrysanthemum that possesses some of these features in order to model ornamental quality in response to abiotic conditions. Only few studies have incorporated and visualized 3D plant structures in mechanistic growth models up to now (for an overview, see Godin and Sinoquet 2005). Especially the L-system formalism is able to generate detailed, realistically visualized 3D plants in interaction with their 3D environment, which are referred to as ‘virtual plants’ (e.g. Měch and Prusinkiewicz 1996). This approach is used in this study for cut chrysanthemum, cultivar ‘Reagan Improved’ and extended with rules from process-based physiological models. Recent studies show that simultaneous modelling of structures and functions can explicitly simulate the effects of local processes on the plant and crop level (Drouet and Pagès 2003; Hanan and Hearn 2003). In this paper, such a combination is used for light and temperature effects on development and growth of individual organs. The model was parameterized for a growth trial under controlled conditions. Its potential to simulate the effect of varying environmental conditions on plant growth and, possibly, ornamental quality is validated in a greenhouse trial. The pros and cons of one model that integrates multiple environmental processes in plant form and functioning is discussed in relation to its increasing complexity.

MODEL DESCRIPTION

General

The model consists of three modules (Figure 1):

- An architectural module, describing the spatial relation and development of the plant organs in terms of symbols, according to the L-alphabet (e.g. Měch and Prusinkiewicz 1996). This results in a full 3D description of the plant in its environment. This module has a time-step of one day.
- A light-radiosity module, which takes as input the 3D scene, including the position and intensity of photosynthetically active radiation (PAR) of the light sources. Rays are emitted from the light sources and are traced throughout the 3D scene. The model used is the nested radiosity, developed by Chelle and Andrieu (1998). The model output is the absorbed PAR by each leaf. This module has a time-step of one hour.
- A carbon module, which consists of two sub-modules:
 1. an assimilation module according to the biochemical model of Farquhar, which calculates the hourly amount of assimilates produced per leaf
 2. a sink–source module, which takes into account the maintenance respiration and the assimilate distribution over the various plant organs according to a relative sink-strength model. The hourly assimilation per leaf is aggregated to plant level each day and distributed over the plant.

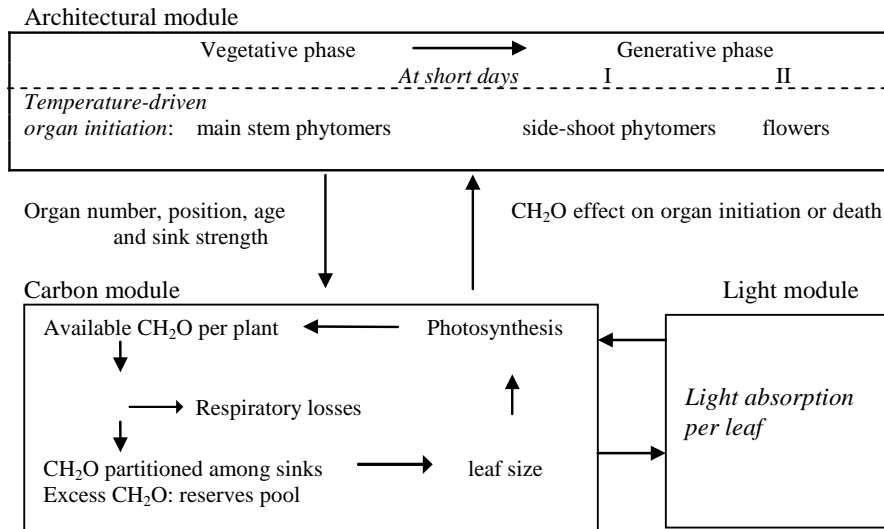


Figure 1. Model structure and links between modules; environmental influences in italics

Inputs

Environmental conditions are supplied to the model as hourly readings of light intensity and spatial position, and greenhouse-averaged temperature, CO_2 concentration and relative humidity. The model supports light input of several spectral bands. For the current model, light is confined to photosynthetically active radiation (PAR in $\mu\text{mol photons m}^{-2} \text{s}^{-1}$) as calculated from global radiation. From the hourly data, the daily night length (number of hours below a certain light level) is determined, which is relevant for inducing the generative phase of this short-day plant species. To arrive at a mean daylight temperature from hourly data, we defined day temperature as the 90%-percentile of hours with light levels sufficient for growth.

Light interception

PAR is calculated as a fraction of global radiation being either diffuse or direct, depending on the degree of cloudiness (see Gijzen 1994). Directions of the light sources are calculated from the sun's position at the hemisphere at direct light and from 12 representative positions in the sky at diffuse light conditions. If assimilation light is present, its source is located in zenith. The L-system receives data on light level per leaf from the coupled nested radiosity model of Chelle and Andrieu (1998), which is able to do a radiosity calculation for some plants and use a turbid-medium approach for the surrounding canopy. For the current model, multiple scattering is

calculated using full radiosity without nesting on a stand of 25 plants, where the middle plant is assumed representative for a plant in a homogeneous crop stand.

Photosynthesis

Photosynthesis is calculated according to the biochemical model of Farquhar et al. (1980) on the basis of absorbed light, CO₂ and temperature at hourly intervals. The parameters of the model were derived from measured light-response curves at crop level by Körner (2003) on the same cultivar of chrysanthemum. Temperature sensitivity of potential electron transport rate J_{max} ($\mu\text{mol electrons } \mu\text{mol}^{-1} \text{ photons}$) is simply modelled by: $J_{max} = J_{max_{T_{25}}} * T_{air} / 25$, where T_{air} is air temperature (°C). The carboxylation process is calculated according to Evans and Farquhar (1991), using the actual value of J of the Farquhar model and a chloroplast CO₂ concentration equal to $0.67 * [\text{CO}_2]_{air}$ and a CO₂ compensation point in the dark equal to $1.7 * T_{air}$ (Evans and Farquhar 1991). This simplification avoids a complex simulation of internal CO₂ concentration under influence of stomatal opening.

Development

The architectural model starts by generating an L-system of a crop of 25 conventional, young stem cuttings of a mother plant, which carry eight visible leaves and 12 'hidden' phytomers, not visible by eye. Each day the model decides whether a new apical phytomer will appear, in dependence of the elapsed thermal time. For chrysanthemum each new phytomer comprises one internode, one leaf and one axillary bud. Internode elongation rate is dependent on thermal time, but at low assimilate levels elongation is halted to sustain a minimum internode diameter of 6 mm. A base temperature of 0 °C (Larsen and Gertsson 1992) and an optimal temperature for growth of 20 °C are assumed, the latter being observed for length growth (Carvalho and Heuvelink 2003). The same authors found a quadratic response for (internode) growth to non-optimal temperatures, and this correction factor was used for all organ growth processes. The generative phase starts at the first occurrence of a night length longer than 11 hours. After a time period of 4.3 days at temperatures above 20°C, and a non-linearly increasing time period below this temperature (Adams et al. 1998), flowering is evoked by formation of a terminal flower bud, breaking apical dominance. Observations showed that axillary buds on the main stem developed side shoots simultaneously, at a number depending on plant weight. Yet, higher-positioned side shoots start earlier with flower formation than lower ones, given a lag time between flowering on successive side shoots. This time lag is set at one day per side shoot irrespective of temperature (Spaargaren 1996). Every elongating side shoot will develop one or more flowers, depending on the amount of sugars available for growth, to be determined by inverse modelling or detailed experimentation. In the generative-growth phase, internodes and attached leaves continue to grow until all flowers are initiated.

Carbohydrate dynamics in the plant

The carbohydrates from net photosynthesis of individual leaves are added at plant level to the pool of available carbohydrates, which also includes free available reserves from previous periods. Maintenance respiration is set at 2% of the carbon present in dry matter. Subsequently the sink strength or carbohydrate demand of every single organ is calculated from its thermal age. This demand includes carbohydrates used for structural tissue plus 30% for growth respiration. The course of the organ's sink strength with age is a function of the weighted temperature sum, and can be described reasonably well by a Gompertz curve. The derivative of the Gompertz curve gives the sink strength at a certain unit of thermal time. The sink strength used for this paper is confined to the conditions of the growth-chamber experiment, in which the carbohydrate sink per organ was empirically determined in the period of rapid growth. Although light level was high (370 PAR in $\mu\text{mol photons m}^{-2} \text{ s}^{-1}$, totalling $13.5 \text{ MJ m}^{-2} \text{ day}^{-1}$) and mutual shading was hardly observed, in theory light and thus source limitation may have occurred, implying underestimation of the determined sink strength. The maximum sink strength is assumed not to vary with organ position or ranking in the plant. In analogy to Marcelis et al. (2006), the available carbohydrate sources are distributed in proportion to the relative sink strengths of all individual organs. If on a daily basis source strength exceeds sink strength, all sinks are filled according to their sink strength and the remaining carbohydrates are stored in the reserves pool.

Allometry and 3D structure

The model requires relationships between weight and length and between weight and volume for internodes, between weight and length and between weight and area for leaves, and between weight and area for flowers. The following relations were taken from the growth-chamber trial (De Visser et al. 2006), with weights in g dry matter (DM) for growing organs:

internode:	length (mm)	$= 260 * \text{weight} - 632 * \text{weight}^2$	(i)
	width (mm)	$= 2 + 30 * \text{weight}$	(ii)
leaf:	length(mm)	$= 337 * \text{weight}^{0.48}$	(iii)
	area (mm ²)	$= 329 * \text{weight}$	(iv)
flower:	diameter (mm)	$= 552 * \text{weight} - 882 * \text{weight}^2$	(v)

A mean leaf angle and phyllotaxis of $40^\circ (\pm 15^\circ)$ was taken, as measured with 3D scans, and a phyllotaxis of $135^\circ (\pm 32^\circ)$, determined by hand (see De Visser et al. 2006). Leaf shape and indentation were determined from flatbed scanner data.

PARAMETERIZATION

Calibration data were derived from a growth-chamber experiment, carried out with stem cuttings of chrysanthemum, cultivar Reagan Improved, planted in 12-cm pots

at a density of 69 plants per m². Two temperature treatments were carried out, 16°C and 20°C each in a replicated growth chamber at a relative humidity of 75% (16°C) and 70% (20°C). The experiment lasted 70 (20°C) to 77 (16°C) days. Plants were grown under long-day (LD) conditions for 14 days, followed by short-day (SD) conditions until the end of the experiment. During the LD and SD periods assimilation light of 370 $\mu\text{mol PAR m}^{-2} \text{s}^{-1}$ (at top of plant) was provided for 8 hrs, extended with incandescent lamps (13 μmol) for 11 hrs in LD and 3 hrs in SD period.

Validation was done on data of a greenhouse experiment where cuttings of chrysanthemum, cultivar Reagan Improved were planted at two densities (32 and 64 plants per m²), each density grown at temperature set points of 16 and 20°C. All four treatments were duplicated. Growth started on 4 November 2004 and ended between 24 January and 14 February, depending on the treatment. Assimilation light was provided for 18 and 8 hours in LD and SD periods, respectively, at 44 $\mu\text{mol PAR m}^{-2} \text{s}^{-1}$. Light extinction at diffuse light conditions was measured (n=6) 10 times during crop development.

Collection of plant data

At the start of the experiments, at the end of the LD period, twice during the SD period and at the final harvest, five plants per treatment were harvested for determination of organ length, internode thickness, individual leaf and flower areas, organ fresh and dry weight (dried at 105°C for 48 hours) and leaf shape. 3D structure of the plants was determined by digitization using a Scanstation (ScanBull®, Hameln, Germany) prior to harvest in both experiments and non-destructively on two plants of the growth-chamber experiment during their development. At the end of the experiment, these two plants were harvested and measured as described above.

Sink-strength estimation

The observed rates of biomass increment with thermal time were used to determine the parameters of the sink-strength curve of internodes, leaves and flowers. A 3-parameter asymmetric S-shaped Gompertz curve was fitted to the data of both temperature treatments of the calibration trial. Internode and leaf data on phytomers 9 to 20 of the main stem were used, assuming no competition for carbon sources during organ formation in this exponential growth phase. Since flower growth is not finished when commercially harvested, for its sink function a maximum biomass of 0.21 g DM was assumed (Carvalho 2003).

RESULTS

Plant development

For plants in the growth-chamber experiment, a phyllochron of 33 °Cd was deduced from the observed, constant rate of phytomer appearance in the vegetative phase. Both phyllochron and final number of phytomers were used to estimate the number of phytomers present at the experimental start, as not all were visible by eye. The eight initially visible leaves and internodes showed a constrained growth during the experiment and were not used in the parameterization studies. All leaves and internodes on the main stem stopped growing in weight at approximately 25 days after start of the SD period. This growth stop was incorporated in the model, referring to it as a hormonal influence due to the completion of flower meristem formation.

At plant level, measured differences between temperature treatments were significant for plant height, average internode length and flower biomass (Table 1). There was a trend towards a higher number of flowers, lower leaf mass and leaf area at 20°C relative to 16°C. Both temperature treatments showed an equal number of appearing side shoots. Slightly more flowers were formed per side shoot at the higher-temperature treatment. At the organ level further differences between the two temperatures were observed: internodes were thicker and flowers were slightly heavier at the lower temperature.

Table 1. Observed and modelled plant characteristics at final harvest in the growth chamber. Weights in g dry matter per plant, comparing treatments at 16°C and 20°C. Different letters behind means indicate differences at 5% level between treatments

Plant attribute	16°C		20°C	
	Observed	Model	Observed	Model
Weight leaves	3.1 ± 0.3	2.9	2.8 ± 0.6	2.8
Weight internodes	6.2 ± 1.1	6.1	6.0 ± 1.4	5.9
Weight flowers	2.0 ± 0.4a	2.1	2.8 ± 0.6b	2.8
Total	11.3 ± 1.5	11.1	11.6 ± 2.8	11.5
Plant height (cm)	65 ± 5a	77	76 ± 3b	76
Nr of leaves#	33 ± 1.6	33	33 ± 1.5	33
Nr of flowers	20 ± 4	17	23 ± 7	22

leaves from main stem only

Sink-strength estimation

Leaves reached their maximum growth rate earlier than internodes. The weight increments at phytomers 10 to 20, from which the sink-strength functions were derived, clearly show this pattern (Figure 2). Internode length, leaf length and leaf weight showed comparable patterns of increment over thermal time. However, the

increase in internode weight, and derived sink strength, lagged behind, indicating an increasing specific weight of internodes with thermal time.

Simulated growth pattern at calibration and validation

Reflection and transmission coefficient were adjusted to arrive at good fits between simulated and observed light extinction, giving 15% reflection and 20% transmission of PAR by the topside of leaves. Using the fitted light extinction, the plant model was successfully calibrated on plant level by increasing the value for light-use efficiency by 50%. This resulted in a good fit between observed and simulated plant biomass at final harvest. No further corrections on model parameters were carried out.

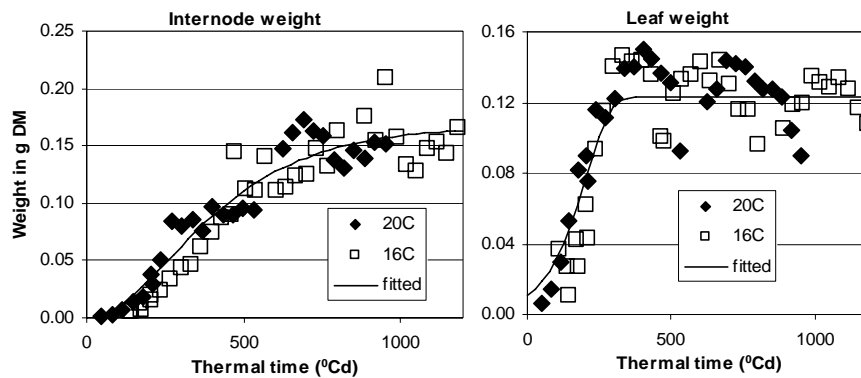


Figure 2. Biomass increment (g dry matter) of organs with thermal time, and fitted to a Gompertz curve. Observed values from the two temperature treatments have different symbols. Explained variances were 95.6 (leaves), 92.0 (internode) and 87.9% (flowers)

At phytomers 10 to 20 on the main stem, the calibration resulted in a reasonable agreement between simulation and observation for weights of individual internodes and leaves (Figure 3) with time. At higher phytomer ranks, simulated leaf and stem growth was stopped at day 25 of the generative phase since all flowers were formed. This resulted in preferential carbohydrate allocation to the flowers (Table 1). Modelling of temperature response showed that the 20°C treatment started flowering earlier, allocated more carbohydrates to flowers and thus had lower leaf and stem biomass in the end than the 16°C treatment. Individual flower weight was approximately equal between temperatures, being related to the constant, temperature-insensitive rate of basipetal flower induction. Unlike the observation, simulated plant height was not different between temperatures because the model allowed length growth to continue until harvest.

Preliminary results of the model validation on the greenhouse trial showed that the model slightly underestimated growth, giving for modelled and observed plant weight, respectively, 4 g and 5 g at 64 plants m⁻² and 6.5 and 8.1 g at 32 plants m⁻².

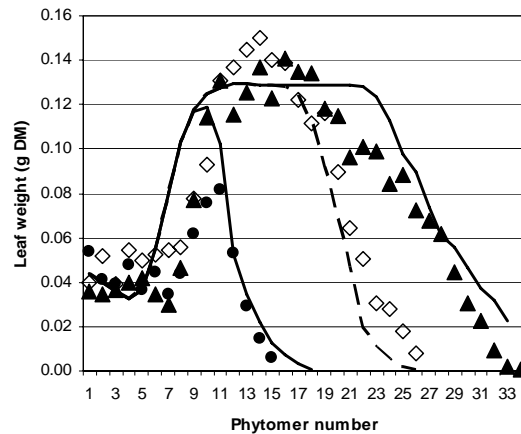


Figure 3. Biomass of individual leaves on days 14 (●), 30 (◇) and 70 (▲) (plant at the right) at 20°C in the growth-chamber experiment. Symbols: observations; lines: simulation

DISCUSSION

The model is able to simulate biomass and dimensions of individual organs for the experimental situation. The simulation of temperature and assimilate effects on plant appearance and ornamental quality in terms of stem width, stem height and flower size was reasonable. Model validation showed that modelled growth rates were lower than observed, yet light level was exceptionally low (<7 MJ m⁻² day⁻¹). This may have attributed to lower maintenance losses than modelled. Low losses were reported for chrysanthemum by Acock et al. (1979) for older tissues and by Lee and Heuvelink (2003) for conditions of low assimilate supply. For a more general applicability, the model's behaviour has to be explored further under a range of growth conditions.

Our use of simulated 3D light absorption at leaf level might not be required since our model pools the produced assimilates at plant level. Moreover, a 3D light model like the applied radiosity method requires complicated measurements on direction and intensity of the light sources and subsequent interception by the plant. Yet, modelling local differences in light absorption per leaf can potentially be helpful to explain effects of local situations on development of chrysanthemum, e.g., the appearance of axillary shoots.

We dealt with only a few levels of light and temperature, and realize that further improvements are required to make the model of practical value. Moreover, interactions between radiation and temperature are difficult to quantify, e.g., at

higher radiation levels, sensitivity to higher temperature decreases, or, at lower radiation levels, start of flower initiation is retarded at low temperature (Karlsson et al. 1989). Nevertheless, the model can be advocated as an attractive and innovative tool because now ornamental quality can be visualized in 3D.

REFERENCES

- Acocck, B., Charles-Edwards, D.A. and Sawyer, S., 1979. Growth response of a Chrysanthemum crop to the environment. III. Effects of radiation and temperature on dry matter partitioning and photosynthesis. *Annals of Botany*, 44 (3), 289-300.
- Adams, S.R., Pearson, S. and Hadley, P., 1998. The effect of temperature on inflorescence initiation and subsequent development in chrysanthemum cv. Snowdon (*Chrysanthemum x morifolium* Ramat.). *Scientia Horticulturae*, 77 (1/2), 59-72.
- Carvalho, S.M.P., 2003. *Effects of growth conditions on external quality of cut chrysanthemum: analysis and simulation*. Wageningen University, Wageningen. PhD thesis Wageningen
- Carvalho, S.M.P. and Heuvelink, E., 2003. Effect of assimilate availability on flower characteristics and plant height of cut chrysanthemum: an integrated study. *Journal of Horticultural Science & Biotechnology*, 78 (5), 711-720.
- Chelle, M. and Andrieu, B., 1998. The nested radiosity model for the distribution of light within plant canopies. *Ecological Modelling*, 111 (1), 75-91.
- De Visser, P.H.B., Van der Heijden, G.W.A.M., Marcelis, L.F.M., et al., 2006. A functional-structural model of chrysanthemum for prediction of ornamental quality. *Acta Horticulturae*, 718, 59-66.
- Drouet, J.L. and Pagès, L., 2003. GRAAL: a model of GRowth, Architecture and carbon ALlocation during the vegetative phase of the whole maize plant: model description and parameterisation. *Ecological Modelling*, 165 (2/3), 147-173.
- Evans, J.R. and Farquhar, G.D., 1991. Modelling canopy photosynthesis from the biochemistry of the C3 chloroplast. In: Boote, K.J. and Loomis, R.S. eds. *Modeling crop photosynthesis: from biochemistry to canopy: proceedings of a symposium in Anaheim, California, 29 November 1988*. Crop Science Society of America, Madison, 1-15. CSSA Special Publication no. 19.
- Farquhar, G.D., Von Caemmerer, S. and Berry, J.A., 1980. A biochemical model of photosynthetic CO₂ assimilation in leaves of C3 species. *Planta*, 149 (1), 78-90.
- Gijzen, H., 1994. *Development of a simulation model for transpiration and water uptake and of an integral crop model*. Plant Research International, Wageningen. Report Plant Research International no. 18.
- Godin, C. and Sinoquet, H., 2005. Functional-structural plant modelling. *New Phytologist*, 166 (3), 705-708.
- Hanan, J.S. and Hearn, A.B., 2003. Linking physiological and architectural models of cotton. *Agricultural Systems*, 75 (1), 47-77.
- Karlsson, M.G., Heins, R.D., Erwin, J.E., et al., 1989. Temperature and photosynthetic photon flux influence chrysanthemum shoot development and flower initiation under short-day conditions. *Journal of the American Society for Horticultural Science*, 114 (1), 158-163.
- Körner, O., 2003. *Crop based climate regimes for energy saving in greenhouse cultivation*. Wageningen University, Wageningen. PhD thesis Wageningen [<http://www.library.wur.nl/wda/dissertations/dis3403.pdf>]
- Larsen, R. and Gertsson, U., 1992. Model analysis of shoot elongation in *Chrysanthemum X morifolium*. *Scientia Horticulturae*, 49 (3/4), 277-289.
- Lee, J.H. and Heuvelink, E., 2003. Simulation of leaf area development based on dry matter partitioning and specific leaf area for cut chrysanthemum. *Annals of Botany*, 91 (3), 319-327.
- Marcelis, L.F.M., Elings, A., Bakker, M., et al., 2006. Modelling dry matter production and partitioning in sweet pepper. *Acta Horticulturae*, 718, 121-128.
- Mëch, R. and Prusinkiewicz, P., 1996. Visual models of plants interacting with their environment. In: *Proceedings of the 23rd annual conference on Computer graphics and interactive techniques*. SIGGRAPH, New Orleans, 397-410.
- Spaargaren, J.J., 1996. *The year round production of Chrysanthemum (in Dutch)*. Applied Plant Research, Aalsmeer.